

Article

# Structurally Characterized Solvent-Induced Homotrimeric Cobalt(II) N<sub>2</sub>O<sub>2</sub>-Donor Bisoxime-Type Complexes

Xiu-Yan Dong, Quan-Peng Kang, Xiao-Yan Li, Jian-Chun Ma and Wen-Kui Dong \* 

School of Chemical and Biological Engineering, Lanzhou Jiaotong University, Lanzhou 730070, China; dxy568@163.com (X.-Y.D.); KQpeng2580@163.com (Q.-P.K.); L1401569787@163.com (X.-Y.L.); majc0204@126.com (J.-C.M.)

\* Correspondence: dongwk@126.com; Tel.: +86-931-4938-703

Received: 22 February 2018; Accepted: 15 March 2018; Published: 19 March 2018

**Abstract:** Four new solvent-induced Co(II) complexes with chemical formulae  $[\{\text{CoL}(\mu_2\text{-OAc})(\text{MeOH})\}_2\text{Co}]$  (**1**),  $[\{\text{CoL}(\mu_2\text{-OAc})(\text{EtOH})\}_2\text{Co}]$  (**2**),  $[\{\text{CoL}(\mu_2\text{-OAc})(\text{Py})\}_2\text{Co}]$  (**3**) and  $[\{\text{CoL}(\mu_2\text{-OAc})(\text{DMF})\}_2\text{Co}]$  (**4**) ( $\text{H}_2\text{L} = 4\text{-nitro-4'-chloro-2,2'-}[(1,3\text{-propylene})\text{dioxybis}(\text{nitrilomethylidene})]\text{diphenol}$ ) have been synthesized and characterized by elemental analyses, FT-IR, UV-Vis spectra and single-crystal X-ray diffraction. Each of the prepared complexes, crystallizing in the space groups  $P-1$  (**1** and **4**),  $P2_1/n$  (**2**) and  $P2_1/c$  (**3**), consists of three Co(II) atoms, two completely deprotonated  $(\text{L})^{2-}$  units, two  $\mu_2$ -acetato ligands and two coordinated solvent molecules. Although the four complexes **1–4** were synthesized in different solvents, it is worthwhile that the Co(II) atoms in the four complexes **1–4** adopt hexa-coordinated with slightly distorted octahedral coordination geometries, and the ratio of the ligand  $\text{H}_2\text{L}$  to Co(II) atoms is 2:3. The complexes **2–4** possess a self-assembled infinite 1D, 2D and 1D supramolecular structures via the intermolecular hydrogen bonds, respectively. Magnetic measurement was performed in the complex **3**.

**Keywords:** N<sub>2</sub>O<sub>2</sub>-donor bisoxime-type complex; synthesis; structure; solvent effect; magnetic property

## 1. Introduction

Salen-type ligands ( $\text{R-CH=N}-(\text{CH}_2)_n\text{-N=CH-R}$ ) and their metal complexes have been extensively investigated in modern coordination chemistry for several decades [1–5]. The reaction of salicylaldehyde or its derivatives with diamines is easy to obtain Salen-type N<sub>2</sub>O<sub>2</sub> ligands, and which could react with transition metal ions to obtain stable mono- or polynuclear complexes [6–10]. Their metal complexes are used as catalysts [11], optical materials [12–19], molecular recognitions [20–23], supramolecular architectures [24–32], biological fields [33–37], magnetic materials [38–43] and so forth.

To date, Salamo-type ligand as a novel Salen-type analogue has been studied originally. Salamo-type ligand ( $\text{R-CH=N-O}-(\text{CH}_2)_n\text{-O-N=CH-R}$ ) is one of the most versatile ligands and the large electronegativity of oxygen atoms is expected to strongly affect the electronic properties of the N<sub>2</sub>O<sub>2</sub> coordination sphere, which can lead to different and novel structures and properties of the resulting complexes. Owing to the unique structures of Salamo-type complexes, a study was shown that it is at least 104 times more stable than Salen-type complexes [44].

Herein, we report the syntheses, crystal structures and solvent effects of four homotrimeric Co(II) complexes,  $[\{\text{CoL}(\mu_2\text{-OAc})(\text{MeOH})\}_2\text{Co}]$  (**1**),  $[\{\text{CoL}(\mu_2\text{-OAc})(\text{EtOH})\}_2\text{Co}]$  (**2**),  $[\{\text{CoL}(\mu_2\text{-OAc})(\text{Py})\}_2\text{Co}]$  (**3**) and  $[\{\text{CoL}(\mu_2\text{-OAc})(\text{DMF})\}_2\text{Co}]$  (**4**). ( $\text{H}_2\text{L} = 4\text{-Nitro-4'-chloro-2,2'-}[(1,3\text{-}$

propylene)dioxybis(nitrogenylmethylidene)]diphenol). Compared with the previously reported complexes, the complexes 1–4 have similar symmetrically trinuclear structures. The content of the present work is mainly studied the crystal structures, solvent effects and magnetic property. With respect to these complexes, phenoxo bridging plays a key role in assembling metal ions and Salamo-type ligands. As shown in complex 1, O1 or O2 as phenoxo atom, bridges Co(II) atoms and Salamo-type ligands, and two Co(II) atoms are also bridged through the  $\mu_2$ -acetato ligand. The  $\mu_2$ -acetato ligand has a strong chelating abilities, can form more stable complex so as to better study its properties.

## 2. Experimental Section

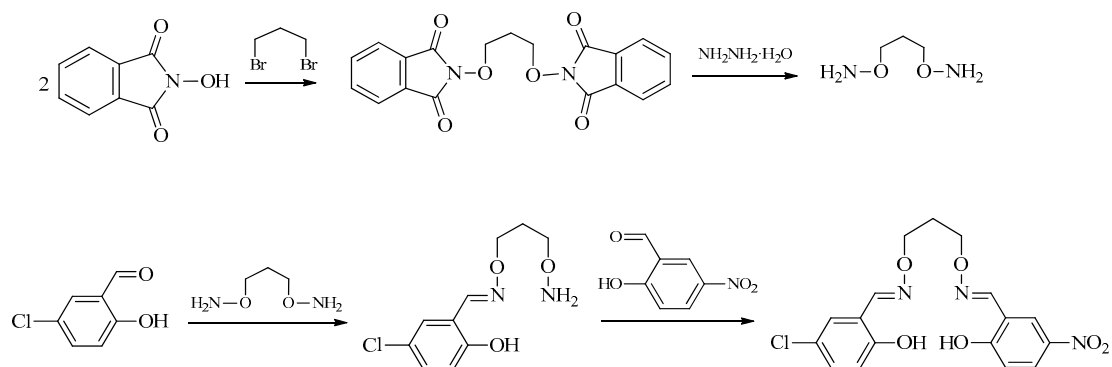
### 2.1. Materials and Methods

5-Chlorosalicylaldehyde and 5-nitrosalicylaldehyde of 98% was purchased from Alfa Aesar (New York, NY, USA) and have been used without further purification. 1,3-Dibromopropane and other reagents were analytical grade reagents from Tianjin Chemical Reagent Factory.

C, H, and N analyses were obtained using a GmbH VarioEL V3.00 automatic elemental analysis instrument (Elementar, Berlin, Germany). Elemental analysis for Co was carried out by an IRIS ER/SWP-1 ICP atomic emission spectrometer (Elementar, Berlin, Germany). Melting points were obtained by the use of a microscopic melting point apparatus made in Beijing Taike Instrument Limited Company (Beijing, China) and were uncorrected. IR spectra were recorded on a VERTEX70 FT-IR spectrophotometer (Bruker, Billerica, MA, USA), with samples prepared as KBr pellets, in the region 3500–400  $\text{cm}^{-1}$ . UV-Vis absorption spectra were recorded on a Shimadzu UV-3900 spectrometer (Shimadzu, Tokyo, Japan).  $^1\text{H}$  NMR spectra were determined by German Bruker AVANCE DRX-400 spectrometer (Bruker AVANCE, Billerica, MA, USA). Single-crystal X-ray structure determinations for the complexes 1–4 were carried out on a SuperNova Dual Eos (Cu at zero) four-circle or Bruker Smart Apex CCD (Bruker AVANCE, Billerica, MA, USA) diffractometer. Magnetic susceptibility was collected by using a Quantum Design model MPMS XL7 SQUID magnetometer (San Diego, CA, USA).

### 2.2. Synthesis and Characterization of $\text{H}_2\text{L}$

The main reaction steps involved in the synthesis of  $\text{H}_2\text{L}$  are given in Scheme 1. 1,3-Bis(aminooxy)propane was synthesized according to an analogous method reported earlier [18].



**Scheme 1.** The synthetic route of  $\text{H}_2\text{L}$ .

The Salamo-type  $\text{N}_2\text{O}_2$  ligand  $\text{H}_2\text{L}$  was synthesized according a procedure from the literature [44]. To an ethanol solution (80 mL) of 5-chlorosalicylaldehyde (626.0 mg, 4.0 mmol) was added an ethanol solution (50 mL) of 1,3-bis(aminooxy)propane (637.0 mg, 6.0 mmol). The mixture solution was heated at 50–55  $^\circ\text{C}$  for 5 h. The solution was concentrated in vacuo and the residue was purified by column chromatography ( $\text{SiO}_2$ , chloroform/ethyl acetate, 10:1) to afford colorless flocculent crystalline solid of

2-hydroxy-5-chlorobenzaldehyde *O*-(2-(aminoxy)ethyl) oxime (655.0 mg, 2.68 mmol). Yield, 66.9%. Anal. Calcd. for C<sub>10</sub>H<sub>13</sub>ClN<sub>2</sub>O<sub>3</sub> (%): C, 49.09; H, 5.36; N, 11.45. Found: C, 49.31; H, 5.47; N, 11.22.

A solution of 2-hydroxy-5-chlorobenzaldehyde *O*-(2-(aminoxy)ethyl) oxime (489 mg, 2.0 mmol) in ethanol (15 mL) was added to a solution of 5-nitrosalicylaldehyde (334 mg, 2.0 mmol) in ethanol (10 mL). The mixture was stirred at 55–60 °C for 5 h. After cooling to room temperature, the precipitates were collected. The product was dried in *vacuo*, and an orange red powder solid was obtained. Yield, 541 mg (68.8%). m.p. 117–118 °C. <sup>1</sup>H NMR (400 MHz, CDCl<sub>3</sub>) δ 2.18 (t, *J* = 6.0 Hz, 2H, CH<sub>2</sub>), 4.35 (m, 4H, CH<sub>2</sub>), 6.91 (d, *J* = 4.0 Hz, 1H, ArH), 7.04 (d, *J* = 6.0 Hz, 1H, ArH), 7.13 (s, 1H, ArH), 7.23 (dd, *J* = 8 Hz, 1H, ArH), 8.14 (d, *J* = 4.0 Hz, 1H, ArH), 8.16 (s, 1H, ArH), 8.19 (s, 1H, CH=N), 8.26 (s, 1H, CH=N), 9.77 (s, 1H, OH), 10.65 (s, 1H, OH). IR (KBr, cm<sup>-1</sup>): 3084 (w, ν<sub>O-H</sub>), 1613 (s, ν<sub>C=N</sub>), 1263 (s, ν<sub>Ar-O</sub>). UV-Vis (EtOH): λ<sub>max</sub> (ε<sub>max</sub>) 219, 267 and 311 nm. (1 × 10<sup>-5</sup> M). Anal. Calcd. for C<sub>17</sub>H<sub>16</sub>ClN<sub>3</sub>O<sub>6</sub> (%): C, 51.77; H, 4.21; N, 10.59, Found: C, 51.95; H, 4.10; N, 10.37.

### 2.3. Syntheses of the Co(II) Complexes 1–4

#### 2.3.1. [(CoL(μ<sub>2</sub>-OAc)(MeOH))<sub>2</sub>Co] (1)

A methanol solution (3 mL) of Co(OAc)<sub>2</sub>·4H<sub>2</sub>O (3.74 mg, 0.015 mmol) was added dropwise to a acetone solution (1 mL) of H<sub>2</sub>L (3.93 mg, 0.010 mmol) at room temperature. The color of the mixed solution turned to purplish red immediately. After stirring for 10 min at room temperature, the mixture was filtered and the filtrate was allowed to stand at room temperature for about one week, the solvent partially evaporated and purplish red block-like single crystals suitable for X-ray crystallographic analysis were obtained. Yield, 3.06 mg (53.5%). UV-Vis (EtOH): λ<sub>max</sub> (ε<sub>max</sub>) 229 and 368 nm. (1.0 × 10<sup>-5</sup> M). IR (KBr, cm<sup>-1</sup>): 2974 (w, ν<sub>O-H</sub>), 1603 (s, ν<sub>C=N</sub>), 1571 (s, ν<sub>asCOO<sup>-</sup></sub>), 1423 (s, ν<sub>sCOO<sup>-</sup></sub>), 1242 (w, ν<sub>Ar-O</sub>). Anal. Calcd. for C<sub>40</sub>H<sub>42</sub>Cl<sub>2</sub>N<sub>6</sub>Co<sub>3</sub>O<sub>18</sub> (%): C, 42.05; H, 3.71; N, 7.36; Co, 15.47. Found: C, 42.28; H, 3.65; N, 7.17; Co, 15.23.

#### 2.3.2. [(CoL(μ<sub>2</sub>-OAc)(EtOH))<sub>2</sub>Co] (2)

A ethanol solution (3 mL) of Co(OAc)<sub>2</sub>·4H<sub>2</sub>O (3.74 mg, 0.015 mmol) was added dropwise to a acetone solution (1 mL) of H<sub>2</sub>L (3.93 mg, 0.010 mmol) at room temperature. The color of the mixed solution turned to purplish red immediately. After stirring for 10 min at room temperature, the mixture was filtered and the filtrate was allowed to stand at room temperature for about one week, the solvent partially evaporated and purplish red block-like single crystals suitable for X-ray crystallographic analysis were obtained. Yield, 3.61 mg (62.2%). UV-Vis (EtOH): λ<sub>max</sub> (ε<sub>max</sub>) 232 and 372 nm. (1.0 × 10<sup>-5</sup> M). IR (KBr, cm<sup>-1</sup>): 1602 (s, ν<sub>C=N</sub>), 1552 (s, ν<sub>asCOO<sup>-</sup></sub>), 1422 (s, ν<sub>sCOO<sup>-</sup></sub>), 1242 (w, ν<sub>Ar-O</sub>). Anal. Calcd. for C<sub>42</sub>H<sub>36</sub>Cl<sub>2</sub>N<sub>6</sub>Co<sub>3</sub>O<sub>18</sub> (%): C, 43.47; H, 3.13; N, 7.24; Co, 15.24. Found: C, 43.85; H, 3.25; N, 7.11; Co, 15.10.

#### 2.3.3. [(CoL(μ<sub>2</sub>-OAc)(Py))<sub>2</sub>Co] (3)

A methanol solution (3 mL) of Co(OAc)<sub>2</sub>·4H<sub>2</sub>O (3.74 mg, 0.015 mmol) was added dropwise to a acetone solution (1 mL) of H<sub>2</sub>L (3.93 mg, 0.010 mmol) and then methanol solution (0.5 mL) of Py (0.015 mmol) was added. The purplish red mixture was filtered and the filtrate was allowed to stand at room temperature for about one week, the solvent partially evaporated and purplish red block-like single crystals suitable for X-ray crystallographic analysis were obtained. Yield, 3.15 mg (50.9%). UV-Vis (EtOH): λ<sub>max</sub> (ε<sub>max</sub>) 233 and 372 nm. (1.0 × 10<sup>-5</sup> M). IR (KBr, cm<sup>-1</sup>): 1602 (s, ν<sub>C=N</sub>), 1566 (s, ν<sub>asCOO<sup>-</sup></sub>), 1419 (s, ν<sub>sCOO<sup>-</sup></sub>), 1249 (w, ν<sub>Ar-O</sub>). Anal. Calcd. for C<sub>48</sub>H<sub>44</sub>Cl<sub>2</sub>N<sub>8</sub>Co<sub>3</sub>O<sub>16</sub> (%): C, 46.62; H, 3.59; N, 9.06; Co, 14.30. Found: C, 46.79; H, 3.66; N, 8.95; Co, 14.12.

#### 2.3.4. [(CoL(μ<sub>2</sub>-OAc)(DMF))<sub>2</sub>Co] (4)

A methanol solution (2 mL) Co(OAc)<sub>2</sub>·4H<sub>2</sub>O (3.74 mg, 0.015 mmol) was added dropwise to a mixture solution of acetone (1 mL) and DMF (0.5 mL) of H<sub>2</sub>L (3.93 mg, 0.010 mmol). The purplish red

mixture was filtered and the filtrate was allowed to stand at room temperature for a week, the solvent partially evaporated and purplish red block-like single crystals suitable for X-ray crystallographic analysis were obtained. Yield, 2.93 mg (47.8%). UV-Vis (EtOH):  $\lambda_{\max}$  ( $\epsilon_{\max}$ ) 232 and 371 nm. ( $1.0 \times 10^{-5}$  M). IR (KBr,  $\text{cm}^{-1}$ ): 1618 (s,  $\nu_{\text{C=N}}$ ), 1558 (s,  $\nu_{\text{asCOO}^-}$ ), 1417 (s,  $\nu_{\text{sCOO}^-}$ ), 1251 (w,  $\nu_{\text{Ar-O}}$ ). Anal. Calcd. for  $\text{C}_{44}\text{H}_{48}\text{Cl}_2\text{N}_8\text{Co}_3\text{O}_{18}$  (%): C, 43.15; H, 3.95; N, 9.15; Co, 14.44, Found: C, 43.42; H, 3.99; N, 9.05; Co, 14.21.

#### 2.4. Crystal Structure Determination

The single crystals of the Co(II) complexes **1–4** with approximate dimensions of  $0.19 \times 0.22 \times 0.25$ ,  $0.21 \times 0.17 \times 0.14$ ,  $0.13 \times 0.17 \times 0.20$  and  $0.14 \times 0.17 \times 0.19$  mm were placed on a SuperNova, Dual (Cu at zero) Eos. diffractometer or Bruker Smart diffractometer equipped with Apex CCD area detector, respectively. The diffraction data were collected using a graphite monochromated Mo K $\alpha$  radiation ( $\lambda = 0.71073$  Å), respectively. The structures were solved by using the program SHELXS-97 [45] and Fourier difference techniques, and refined by full-matrix least-squares method on  $F^2$  [45]. All hydrogens were added theoretically. Crystallographic data and refinement for all of the Co(II) complexes are summarized in Table 1.

**Table 1.** Crystallographic data and refinement parameter for the Co(II) complexes **1–4**.

Compound Code	1	2	3	4
Empirical formula	$\text{C}_{40}\text{H}_{42}\text{Cl}_2\text{Co}_3\text{N}_6\text{O}_{18}$	$\text{C}_{42}\text{H}_{36}\text{Cl}_2\text{Co}_3\text{N}_6\text{O}_{18}$	$\text{C}_{48}\text{H}_{44}\text{Cl}_2\text{Co}_3\text{N}_8\text{O}_{16}$	$\text{C}_{44}\text{H}_{48}\text{Cl}_2\text{Co}_3\text{N}_8\text{O}_{18}$
Formula weight	1142.49	1160.46	1236.60	1224.59
Temperature (K)	296(2)	294(2)	296(2)	296(2)
Wavelength (Å)	0.71073	0.71073	0.71073	0.71073
Crystal system	triclinic	monoclinic	monoclinic	triclinic
Space group	$P-1$	$P2_1/n$	$P2_1/c$	$P-1$
Unit cell dimensions				
<i>a</i> (Å)	11.0545(13)	13.3496(7)	11.1889(8)	9.195(13)
<i>b</i> (Å)	11.2647(14)	13.6078(5)	9.4659(7)	12.816(18)
<i>c</i> (Å)	12.9730(16)	15.8972(6)	25.6944(17)	13.814(19)
$\alpha$ (°)	69.274(2)	90	90	69.243(18)
$\beta$ (°)	72.603(2)	106.944(5)	108.125(3)	83.06(2)
$\gamma$ (°)	82.921(2)	90	90	84.178(19)
<i>V</i> (Å <sup>3</sup> )	1441.5(3)	2762.5(2)	2586.3(3)	1.349
<i>Z</i>	1	2	2	1
<i>D<sub>c</sub></i> (g·cm <sup>-3</sup> )	1.316	1.395	1.588	1.348
$\mu$ (mm <sup>-1</sup> )	1.011	1.057	1.132	0.972
<i>F</i> (000)	583	1178	1262	627
Crystal size (mm)	$0.19 \times 0.22 \times 0.25$	$0.21 \times 0.17 \times 0.14$	$0.13 \times 0.17 \times 0.20$	$0.14 \times 0.17 \times 0.19$
$\theta$ Range (°)	1.8–25.0	3.39–26.02	1.7–25.5	1.6–25.2
	$-13 \leq h \leq 9$	$-16 \leq h \leq 14$	$-12 \leq h \leq 13$	$-9 \leq h \leq 11$
Index ranges	$-13 \leq k \leq 13$	$-16 \leq k \leq 16$	$-10 \leq k \leq 11$	$-15 \leq k \leq 15$
	$-15 \leq l \leq 12$	$-12 \leq l \leq 19$	$-31 \leq l \leq 18$	$-13 \leq l \leq 16$
Reflections collected	8022	10789	14683	8008
Unique reflections	5051	5416	4825	5341
<i>R</i> <sub>int</sub>	0.023	0.0557	0.032	0.080
Completeness (%) ( $\theta$ )	99.3 (25.00)	99.5 (25.24)	100 (25.24)	98.70% (25.20)
Data/restraints/parameters	5051/0/309	5416/42/363	4825/12/368	5341/21/331
GOF	1.085	0.992	1.027	1.206
Final <i>R</i> <sub>1</sub> , <i>wR</i> <sub>2</sub> indices	0.0463, 0.1416	0.0642, 0.1363	0.0347, 0.0736	0.1010, 0.2039
<i>R</i> <sub>1</sub> , <i>wR</i> <sub>2</sub> indices (all data)	0.0540, 0.1468	0.1203, 0.1620	0.0495, 0.0799	0.1812, 0.2249
Residuals peak/hole (e Å <sup>-3</sup> )	0.93/−0.46	0.54/−0.35	0.44/−0.43	1.46/−0.38

Supplementary crystallographic data for this paper have been deposited at Cambridge Crystallographic Data Centre (1811845, 1811844, 1811842 and 1811843 for the complexes **1**, **2**, **3** and **4**) and can be obtained free of charge via [www.ccdc.cam.ac.uk/conts/retrieving.html](http://www.ccdc.cam.ac.uk/conts/retrieving.html).

### 3. Results and Discussion

#### 3.1. IR Spectra Analyses

IR spectra of H<sub>2</sub>L and its corresponding Co(II) complexes 1–4 exhibits various bands in the region of 3500–400 cm<sup>−1</sup> region (Figure 1). The spectrum of the ligand H<sub>2</sub>L shows an O–H stretching band at 3084 cm<sup>−1</sup> that belongs to phenolic hydroxyl group. The free ligand exhibits a characteristic C=N stretching band at 1613 cm<sup>−1</sup>, while  $\nu_{C=N}$  of the Co(II) complexes 1–4 are observed at 1603, 1602, 1602, and 1618 cm<sup>−1</sup>, respectively [46]. The shift of this C=N absorption bands by about 10, 11, 11 and 5 cm<sup>−1</sup> on going from the free ligand H<sub>2</sub>L to the Co(II) complexes 1–4, respectively.

The Ar–O stretching band is a strong band at 1268–1213 cm<sup>−1</sup> as reported for similar Salen-type ligands [47,48]. This band is at 1263 cm<sup>−1</sup> for H<sub>2</sub>L, and at 1242, 1242, 1249 and 1251 cm<sup>−1</sup> for the complexes 1–4, respectively. The Ar–O stretching bands are shifted to lower wavenumbers, indicating that the Co–O bonds are formed between the Co(II) atoms and oxygen atoms of phenolic groups [31].

The far-infrared spectra of the Co(II) complexes 1–4 were obtained from 550 to 100 cm<sup>−1</sup> to identify wavenumbers due to the Co–O and Co–N bonds. IR spectra of the Co(II) complexes 1–4 show  $\nu(\text{Co–N})$  (or  $\nu(\text{Co–O})$ ) vibrational absorption bands at 527, 515, 521 and 521 (or 476, 489, 476 and 469) cm<sup>−1</sup>, respectively, which are in consistent with the literature values [49,50].

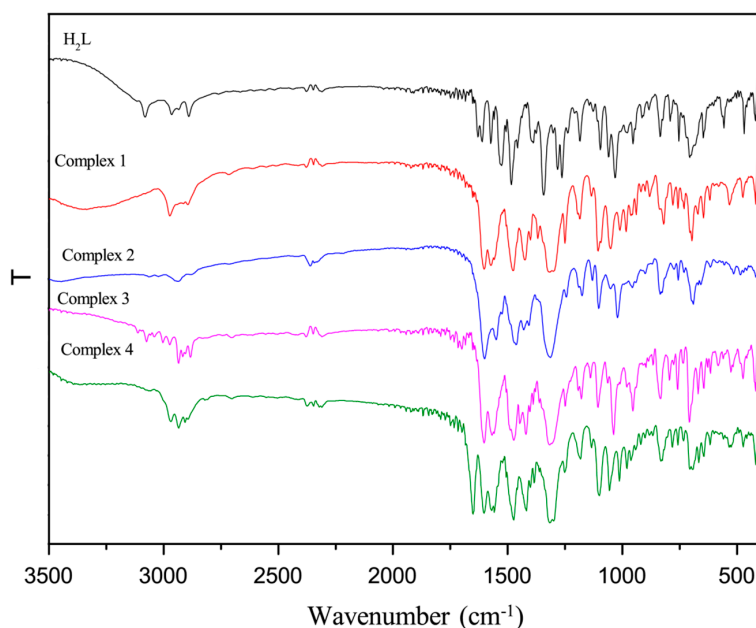


**Figure 1.** Infrared spectra of H<sub>2</sub>L and its complexes 1–4.

#### 3.2. UV–vis Spectra

UV–vis absorption spectra of H<sub>2</sub>L and its complexes 1–4 were determined in  $1.0 \times 10^{-5}$  M ethanol solution, as shown in Table 2 and Figure 2.

**Table 2.** Absorption maxima and molar extinction coefficients for complexes 1–4.

Compound	c			
H <sub>2</sub> L	$1.0 \times 10^{-5}$	219 ( $5.1 \times 10^{-4}$ )	267 ( $4.9 \times 10^{-4}$ )	311 ( $2.6 \times 10^{-4}$ )
Complex 1	$1.0 \times 10^{-5}$	229 ( $1.1 \times 10^{-5}$ )	368 ( $2.6 \times 10^{-4}$ )	
Complex 2	$1.0 \times 10^{-5}$	232 ( $9.5 \times 10^{-4}$ )	372 ( $5.9 \times 10^{-4}$ )	
Complex 3	$1.0 \times 10^{-5}$	233 ( $8.7 \times 10^{-4}$ )	372 ( $5.5 \times 10^{-4}$ )	
Complex 4	$1.0 \times 10^{-5}$	232 ( $5.2 \times 10^{-4}$ )	371 ( $3.4 \times 10^{-4}$ )	

Absorption spectra of the complexes **1–4** show that the complexes **1–4** have similar absorption spectra, but are different from the spectrum of H<sub>2</sub>L. UV-Vis spectrum of H<sub>2</sub>L exhibits three absorption peaks at ca. 219, 267 and 311 nm. The absorptions at 219 and 267 nm can be assigned to  $\pi-\pi^*$  transitions of the benzene rings while the absorptions at 311 nm can be attributed to intraligand  $\pi-\pi^*$  transitions of C=N groups [51–53]. Compared with the absorption peaks of H<sub>2</sub>L, with the emergence of the first absorption peaks at ca. 229–233 nm are observed in the complexes **1–4**. These peaks are bathochromically shifted, indicating coordination of the ligand moieties with Co(II) atoms. The absorption peaks at ca. 267 and 311 nm are absent in the complexes **1–4**. Meanwhile, new absorption peaks are observed at ca. 368–372 nm in the complexes **1–4**, may be due to L→M charge-transfer transitions, which are characteristic of the transition metal complexes with Salen-type N<sub>2</sub>O<sub>2</sub> coordination spheres [54].

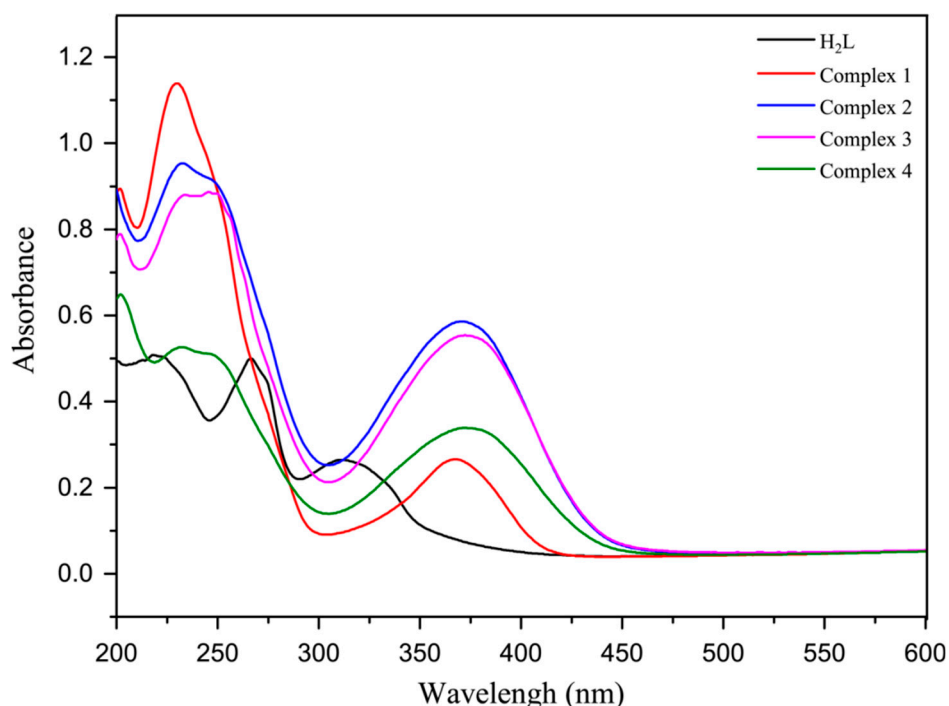


**Figure 2.** UV-vis spectra of H<sub>2</sub>L and its complexes **1–4** in ethanol ( $c = 1.0 \times 10^{-5}$  M).

### 3.3. Description of the Crystal Structures

Selected bond lengths (Å) and angles (°) are presented in Table S1. Hydrogen bonds in the Co(II) complexes **1–4** are given in Table S2.

#### 3.3.1. Structure of the Co(II) Complex **1**

X-ray crystallographic analysis of the Co(II) complex **1** reveals a symmetric trinuclear structure. As depicted in Figure 3. It crystallizes in the triclinic system, space group *P*−1, and consists of three Co(II) atoms, two completely deprotonated (L)<sup>2−</sup> units, two  $\mu_2$ -acetato ligands and two coordinated methanol molecules. All the hexa-coordinated Co(II) atoms lie in slightly distorted octahedral coordination environment. The terminal Co2 atom is hexa-coordinated by two oxime nitrogen (N1 and N2) and two phenolic oxygen (O1 and O2) atoms of the deprotonated Salamo-type (L)<sup>2−</sup> unit, one oxygen (O8) atom comes from the  $\mu_2$ -acetato ligand and the other oxygen (O9) atom comes from the coordinated methanol molecule. The dihedral angle between coordination planes of N1-Co2-O1 and N2-Co2-O2 is 5.03(5)°. This indicates that Co2 forms a slightly distorted octahedral geometry.

The coordination geometry of the central Co1 atom deviates slightly from ideal octahedron. The coordination sphere of the central Co1 atom contains four phenoxo oxygens (O1, O2, O1<sup>#1</sup> and

O2<sup>#1</sup>) atom from two deprotonated (L)<sup>2-</sup> units also coordinated to Co2 atom and double  $\mu_2$ -acetato oxygen (O7 and O7<sup>#1</sup>) atoms that adopts a similar M-O-C-O-M fashion [55,56]. All the six oxygen atoms that are coordinated to Co1 atom constitutes a slightly distorted octahedral geometry [57,58].

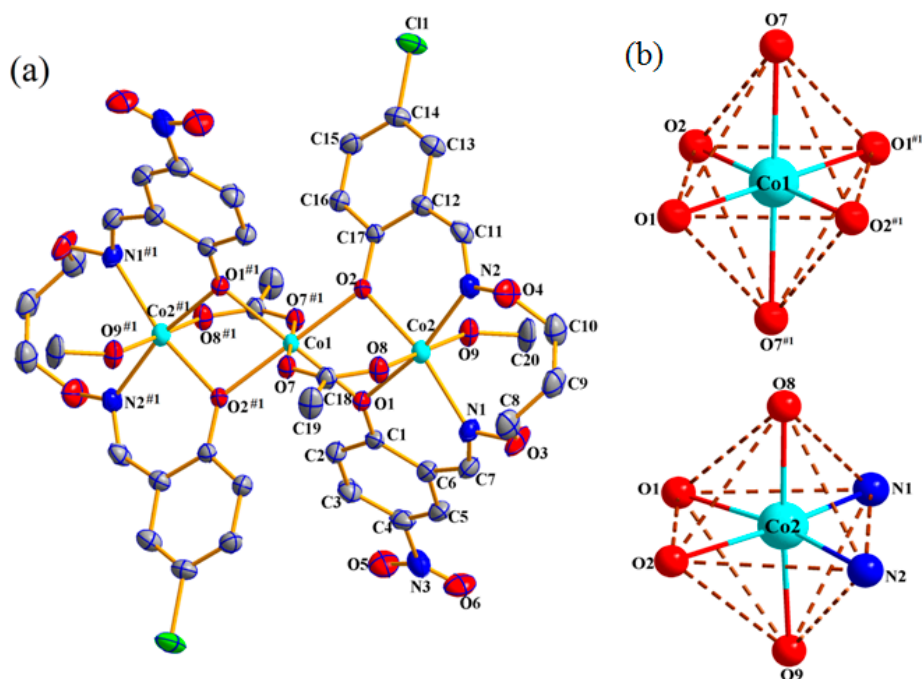


**Figure 3.** (a) Molecular structure and atom numberings of the complex 1 with 30% probability displacement ellipsoids (hydrogen atoms are omitted for clarity); (b) Coordination polyhedra for Co(II) atoms of the complex 1.

In the crystal structure of the complex 1, the structure is connected by three pairs of intramolecular hydrogen bonding (C8–H8A $\cdots$ O8, C10–H10A $\cdots$ O3 and C16–H16 $\cdots$ O7) interactions (Table S2 and Figure 4), which plays a vital role in constructing and stabilizing the complex 1 molecules [59–63].

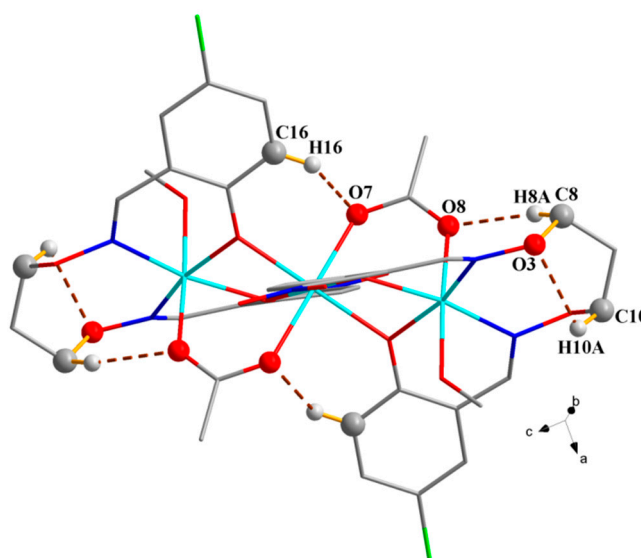


**Figure 4.** View of the intramolecular hydrogen bonds of the complex 1.

### 3.3.2. Structures of the Co(II) Complexes 2–4

X-ray crystal structure analysis of the Co(II) complexes 2–4 indicates that the structure is similar to that of the Co(II) complex 1. They have the same individual trinuclear neutral molecular unit  $[\{CoL(\mu_2-OAc)(solvent)\}_2Co]$  (The solvent molecules are ethanol, Py and DMF in the Co(II) complexes 2–4, respectively), as shown in Figure 5, Figure 6, and Figure 7, respectively, while the different solvents observed lead to the formation of the typical solvent-induced Co(II) complexes [64]. All the hexa-coordinated Co(II) atoms of the Co(II) complexes 2–4 have slightly distorted octahedral coordination polyhedra. The terminal Co2 or Co2<sup>#1</sup> atom lies in a hexa-coordinated environment and adopts a slightly distorted octahedral geometry, where the inner  $N_2O_2$  coordinated environment of the completely pentadentate  $(L)^{2-}$  units comprises the basal plane and one oxygen (O9) atom from the  $\mu_2$ -acetato ligands and one oxygen (O7) atom from the coordinated solvent molecule occupy together the apical positions. (The solvent molecules are ethanol and DMF in the Co(II) complexes 2 and 4, respectively). While for the complex 3, one oxygen (O8) atom from the  $\mu_2$ -acetate ion and one nitrogen (N4) atom from the coordinated Py molecule occupy together the apical positions. The dihedral angle between the two coordination planes of N1–Co2–O1 and N2–Co2–O4 (N2–Co1–O6 and N3–Co1–O5 or N3–Co2–O6 and N2–Co2–O5) is  $7.06(3)^\circ$  in the Co(II) complex 2 ( $6.41(2)$  or  $8.03(2)^\circ$  in the Co(II) complex 3 or 4, respectively), which are larger than the Co(II) complex 1, showing that the terminal Co(II) atoms have higher distortion than the Co(II) complex 1 in octahedral geometries.

In addition, the central Co1 atom is located in a hexa-coordinated environment, surrounded by six oxygen atoms from the two  $[CoL(solvent)]$  units and two oxygen atoms from  $\mu_2$ -acetato ligands, with the same coordination environment as that of the central Co(II) atom in the Co(II) complex 1.

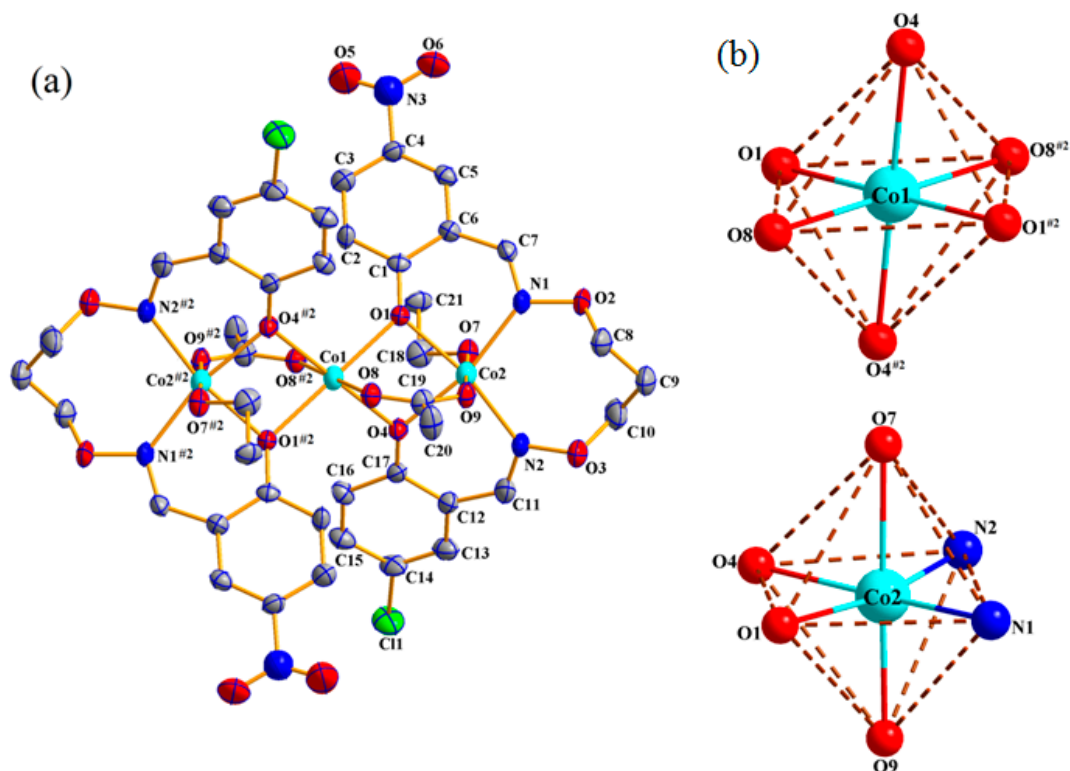


**Figure 5.** (a) Molecular structure and atom numberings of the complex 2 with 30% probability displacement ellipsoids (hydrogen atoms are omitted for clarity); (b) Coordination polyhedra for Co(II) atoms of the complex 2.

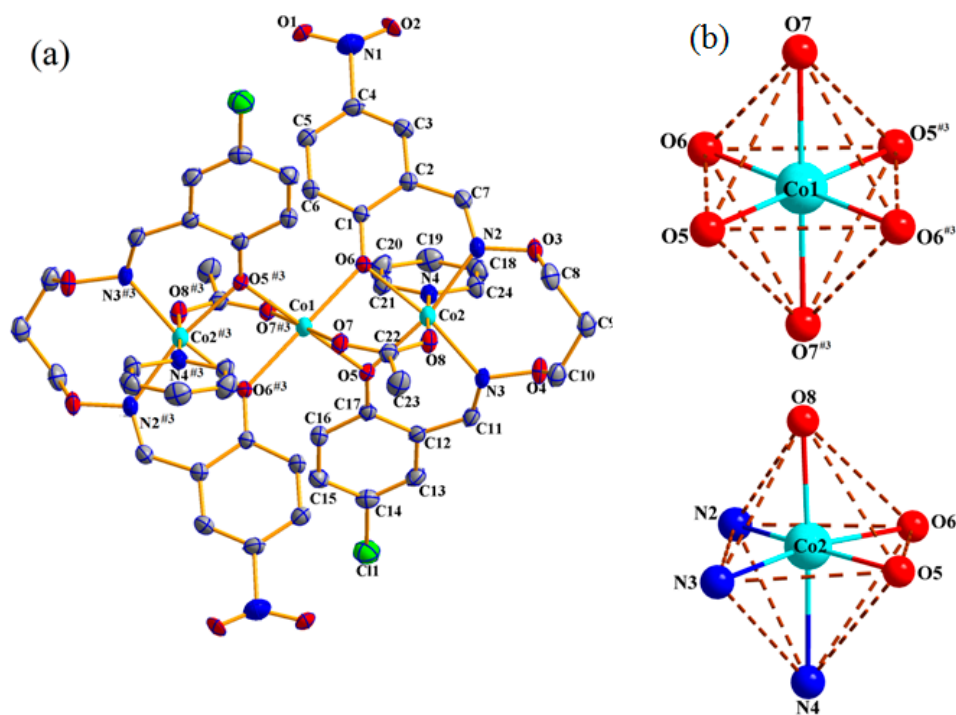


**Figure 6.** (a) Molecular structure and atom numberings of the complex 3 with 30% probability displacement ellipsoids (hydrogen atoms are omitted for clarity); (b) Coordination polyhedra for Co(II) atoms of the complex 3.

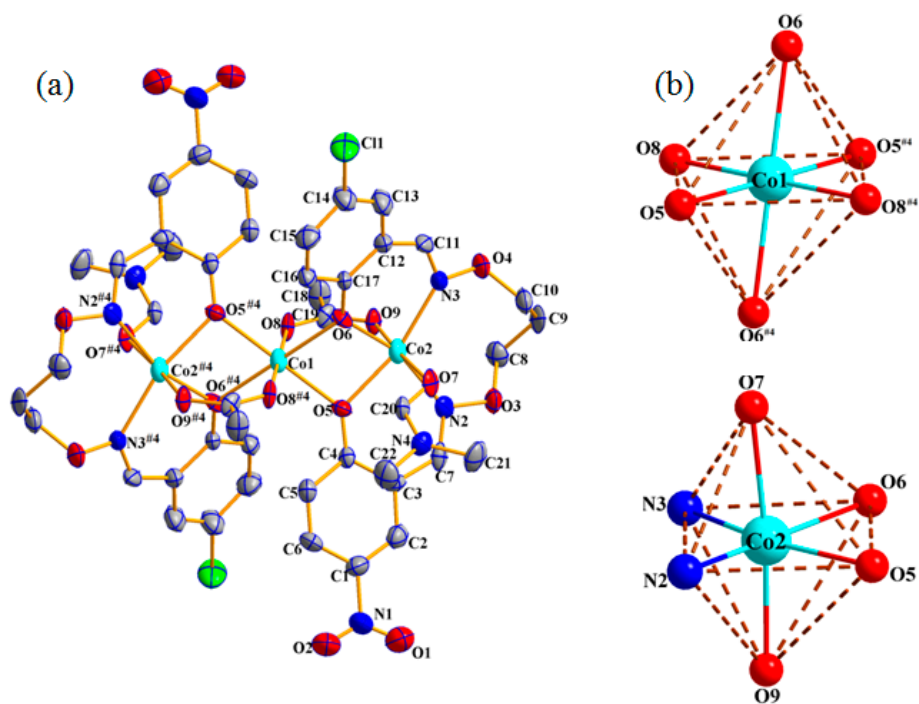


**Figure 7.** (a) Molecular structure and atom numberings of the complex 4 with 30% probability displacement ellipsoids (hydrogen atoms are omitted for clarity); (b) Coordination polyhedra for Co(II) atoms of the complex 4.

It is noteworthy that due to the different coordination solvent molecules of the complexes 1–4, this solvent effect leads to different supramolecular interactions, but all the Co(II) atoms have the

same slightly distorted octahedral geometries, and are shown in blue in the Figures 8b, 9b and 10b. There are three pairs of intramolecular hydrogen bonds in the Co(II) complexes 2 and 3. (C8–H8A···O9, C10–H10A···O2, C18–H18A···O8 and C8–H8B···O8, C10–H10A···O8, C21–H21···O7) (Figures 8a and 9a). The Co(II) complexes 2 and 3 are further linked by a pairs of intermolecular hydrogen bonding interactions form a 1D and 2D supramolecular structures, respectively [65–70], (C5–H5···O6' and C15–H15···O2) (Figures 8b and 9b). In the crystal structure of the complex 4, there are six pairs of intramolecular hydrogen bond (C5–H5···O8, C8–H8B···O9, C10–H10B···O3, C16–H16···O8, C20–H20···O8 and C21–H21C···O7) interactions (Figure 10a). The neighboring complex molecules are linked into an infinite 1D supramolecular structure by intermolecular hydrogen bonding (C22–H22B···O1) interactions (Figure 10b).

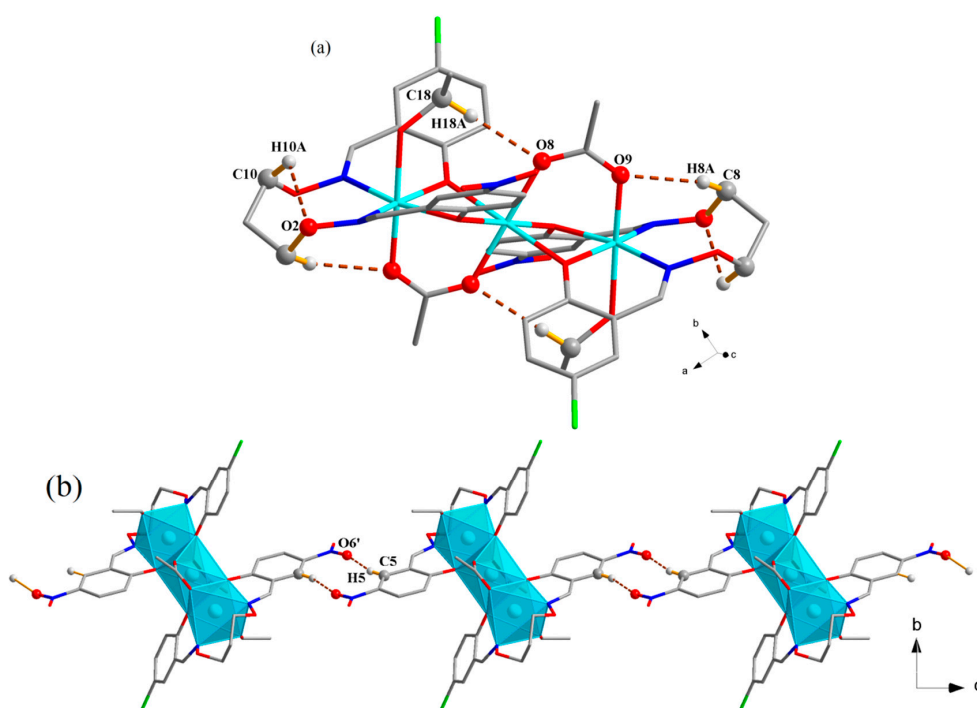


**Figure 8.** (a) View of the intramolecular and (b) intermolecular hydrogen bonds of the complex 2.

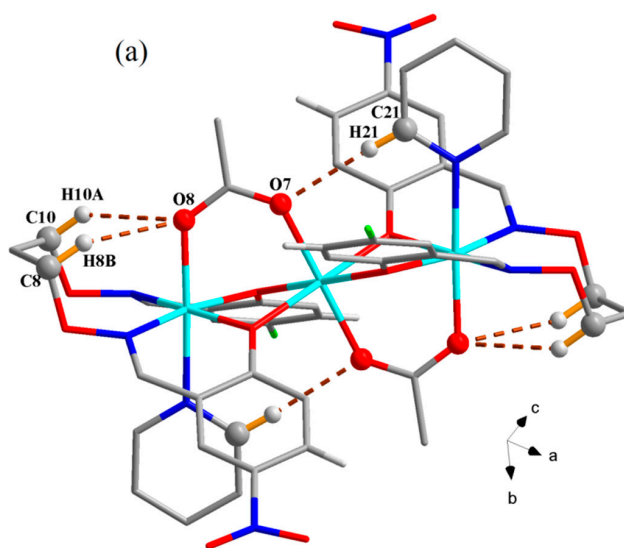


**Figure 9.** Cont.

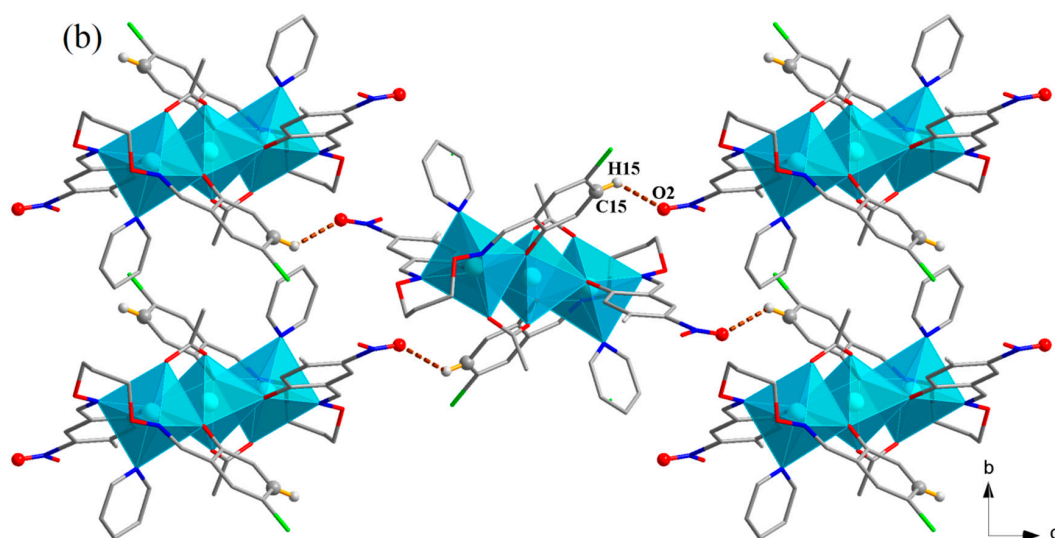


**Figure 9.** (a) View of the intramolecular and (b) intermolecular hydrogen bonds of the complex 3.

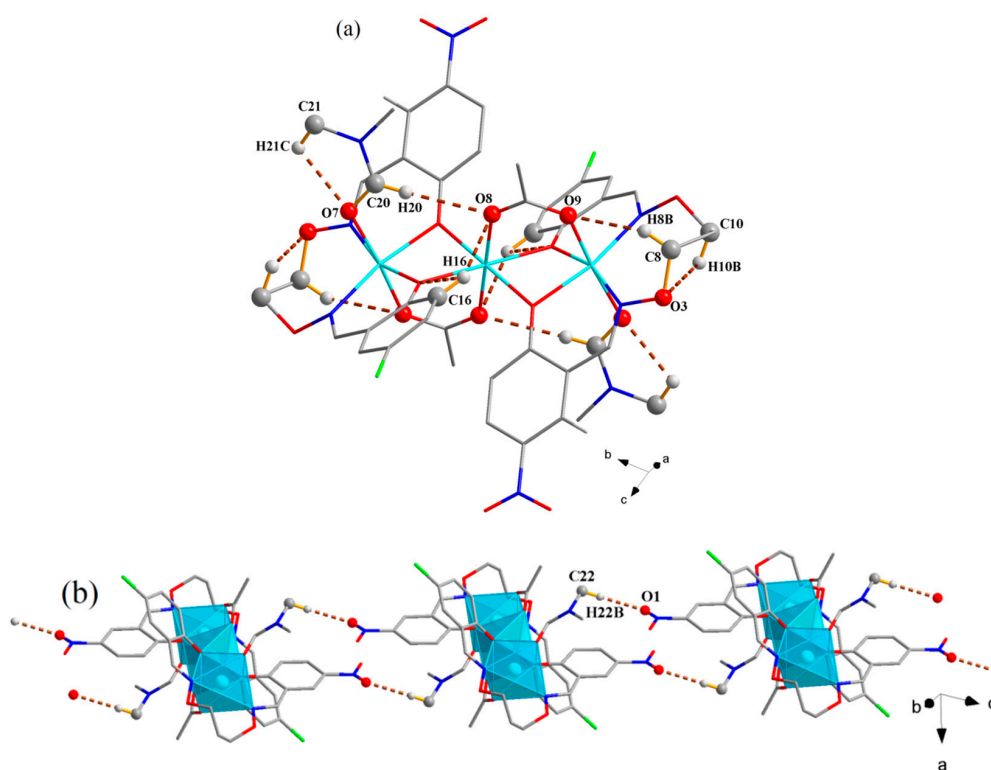


**Figure 10.** (a) View of the intramolecular and (b) intermolecular hydrogen bonds of the complex 4.

To sum up, here we report four homotrimeric Co(II) Salamo-type complexes. In previous reports, the Salamo-type Co(II) complexes are essentially mono- [58], di- [7,31], tri- [11,55,56] and tetra-nuclear [71]. However, trimeric complexes are generally bridged by acetato ligands, and the ratios of the ligand to the Co(II) atoms are 1:1, 2:2, 2:3 and 2:4. Here we have successfully designed and synthesized a new ligand by prolonging length of alkoxy chain of Salamo-type ligand, and including introduce of different aldehyde units. Its corresponding Co(II) complexes were synthesized by the introduction of different solvents, in order to further promote the study of its structure and properties.

### 3.3.3. Solvent Effect

Four Co(II) complexes could be synthesized by the reaction of the Salamo-type ligand  $H_2L$  with  $Co(OAc)_2 \cdot 4H_2O$  in different solvents. The complexes 1–4 present similar stoichiometric ratio when the introduction of different solvent molecules. Although the molecule structures of the Co(II) complexes are similar each other, obtained in different mixture solutions, the complexes 1–4 possess different supramolecular structural features. The Co(II) complexes 2–4 self-assemble into infinite 1D, 2D and 1D supramolecular structures through intermolecular hydrogen bonding interactions, respectively. In the Co(II) complexes 1–4, the solvent effect clearly shows the changes in bond distances (Å) and angles (°). (Table S1). It is noteworthy that the bond lengths from the oxygen (O9 and O7) atoms of the coordinated solvent molecules (methanol or ethanol) to the terminal Co(II) ions in the Co(II) complexes 1 and 2 are 2.109(2) and 2.168(4) Å, respectively, which present a regular elongation when the steric hindrance successively becomes larger from methanol to ethanol.

### 3.4. Magnetic Property

Since complexes 1–4 have similar structures, they have little difference in magnetic properties. This article only discusses the magnetic property of the complex 3. The magnetic analysis of complex 3 was tested under the applied magnetic field of 1000Oe, and the magnetic susceptibility data of the complex 3 in the temperature range of 2–300 K was measured. Measured the sample with the single-crystals of the complex 3. The temperature dependence of magnetic susceptibilities of the complex 3 is shown in Figure 11. The  $\chi_M T$  value of the complex 3 is  $8.79 \text{ cm}^3 \text{ K mol}^{-1}$  at 300 K, which is larger than the value of  $5.63 \text{ cm}^3 \text{ K mol}^{-1}$  expected for three Co(II) ( $S = 3/2$ ) magnetically isolated ions. Upon lowering the temperature, the  $\chi_M T$  value kept decrease gradually to reach a minimum value of  $6.63 \text{ cm}^3 \text{ K mol}^{-1}$  at 10 K, and when the temperature was further decreased, the  $\chi_M T$  value increased sharply and reached a maximum value of  $8.46 \text{ cm}^3 \text{ K mol}^{-1}$  at 2 K. The  $\chi_M T$  value decreased with decreasing temperature, indicating an intramolecular weak antiferromagnetic interaction between the three Co(II) atoms. In addition, when the temperature dropped below 2 K, the sharp increase in the  $\chi_M T$  value is mainly due to the interaction between ferromagnetic molecules, Zero-field splitting and Zeeman effects. The magnetic susceptibilities ( $1/X_M$ ) obey the Curie–Weiss law in the 2–300 K temperature range for the complex 3, giving a negative Weiss constant  $\theta = -6.686 \text{ K}$  and  $C = 8.931 \text{ cm}^3 \text{ K mol}^{-1}$  (Figure 11 inset), and confirming the weak antiferromagnetic interaction exhibited again by the complex 3 [19,43,72–74].

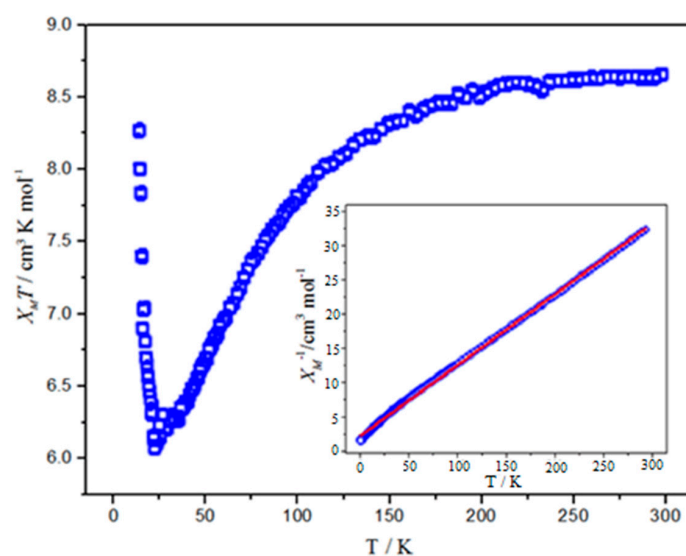


**Figure 11.** Plots of  $\chi_M T$  vs.  $T$  for complex 3 between 2 to 300 K. Inset: Temperature dependence of  $\chi_M^{-1}$ . The red solid lines represent the best fitting results.

#### 4. Conclusions

We have designed and synthesized four new solvent-induced trinuclear Co(II) complexes with a new Salamo-type ligand. Single-crystal X-ray diffraction structures revealed that the structural features of the complexes 1–4 are very similar each other except for the differences in the coordinated solvent molecules. Interestingly, the existence of solvent effect in the complexes 1–4 may be responsible for the slight differences in their crystal and supramolecular structures. The Co(II) complexes 2–4 possess self-assembling infinite 1D, 2D and 1D supramolecular structures via the intermolecular hydrogen bond interactions, respectively. All the Co(II) atoms of the Co(II) complexes 1–4 lie in a hexa-coordinated environment and adopt slightly distorted octahedral geometries. The UV–vis spectra clearly indicate that the structures of the four Co(II) complexes are similar and different from that of the ligand (H<sub>2</sub>L). Magnetic study showed that the complex 3 has weak antiferromagnetic interaction at higher temperature.

**Supplementary Materials:** The following are available online at <http://www.mdpi.com/2073-4352/8/3/139/s1>, Table S1: Selected bond lengths (Å) and angles (°) for the complexes 1–4; Table S2 Hydrogen bonding interactions [Å °] for the complexes 1–4.

**Acknowledgments:** This work was supported by the National Natural Science Foundation of China (21761018) and the Program for Excellent Team of Scientific Research in Lanzhou Jiaotong University (201706), which is gratefully acknowledged.

**Author Contributions:** Wen-Kui Dong conceived and designed the experiments, Xiao-Yan Li performed the experiments; Jian-Chun Ma analyzed the data; Xiu-Yan Dong and Quan-Peng Kang wrote the paper.

**Conflicts of Interest:** The authors declare no competing financial interests.

#### References

1. Sun, Y.X.; Zhang, Y.J.; Meng, W.S.; Li, X.R.; Lu, R.E. Synthesis and crystal structure of new nickel(II) complex with Salen-type bisoxime ligand. *Asian J. Chem.* **2014**, *26*, 416–418.
2. Sun, Y.X.; Xu, L.; Zhao, T.H.; Liu, S.H.; Liu, G.H.; Dong, X.T. Synthesis and Crystal Structure of a 3D Supramolecular Copper(II) Complex With 1-(3-[(E)-3-bromo-5-chloro-2-hydroxybenzylidene amino]phenyl) ethanone Oxime. *Synth. React. Inorg. Met. Org. Nano Met. Chem.* **2013**, *43*, 509–513. [[CrossRef](#)]
3. Chai, L.Q.; Liu, G.; Zhang, Y.L.; Huang, J.J.; Tong, J.F. Synthesis, crystal structure, fluorescence, electrochemical property, and SOD-like activity of an unexpected nickel(II) complex with a quinazoline-type ligand. *J. Coord. Chem.* **2013**, *66*, 3926–3938. [[CrossRef](#)]
4. Song, X.Q.; Peng, Y.Q.; Chen, G.Q.; Wang, X.R.; Liu, P.P. Substituted group-directed assembly of Zn(II) coordination complexes based on two new structural related pyrazolone based Salen ligands: Syntheses, structures and fluorescence properties. *Inorg. Chim. Acta* **2015**, *427*, 13–21. [[CrossRef](#)]
5. Song, X.Q.; Lei, Y.K.; Wang, X.R.; Zhao, M.M.; Peng, Y.Q.; Cheng, G.Q. Lanthanide coordination polymers: Synthesis, diverse structure and luminescence properties. *J. Solid State Chem.* **2014**, *218*, 202–212. [[CrossRef](#)]
6. Chai, L.Q.; Zhang, H.S.; Huang, J.J.; Zhang, Y.L. An unexpected Schiff base-type Ni(II) complex: Synthesis, crystal structures, fluorescence, electrochemical property and SOD-like activities. *Spectrochim. Acta Part A* **2015**, *137*, 661–669. [[CrossRef](#)] [[PubMed](#)]
7. Dong, Y.J.; Dong, X.Y.; Dong, W.K.; Zhang, Y.; Zhang, L.S. Three asymmetric Salamo-type copper(II) and cobalt(II) complexes: Syntheses, structures, fluorescent properties. *Polyhedron* **2017**, *123*, 305–315. [[CrossRef](#)]
8. Sun, Y.X.; Zhang, S.T.; Ren, Z.L.; Dong, X.Y.; Wang, L. Synthesis, Characterization, and Crystal Structure of a New Supramolecular Cd<sup>II</sup> Complex with Halogen-Substituted Salen-Type Bisoxime. *Synth. React. Inorg. Met. Org. Nano Met. Chem.* **2013**, *43*, 995–1000. [[CrossRef](#)]
9. Dong, X.Y.; Akogun, S.F.; Zhou, W.M.; Dong, W.K. Tetranuclear Zn(II) Complex Based on an Asymmetrical Salamo-Type Chelating Ligand: Synthesis, Structural Characterization, and Fluorescence Property. *J. Chin. Chem. Soc.* **2017**, *64*, 412–419. [[CrossRef](#)]
10. Zheng, S.S.; Dong, W.K.; Zhang, Y.; Chen, L.; Ding, Y.J. Four Salamo-type 3d–4f hetero-bimetallic [Zn<sup>II</sup>Ln<sup>III</sup>] complexes: Syntheses, crystal structures, and luminescent and magnetic properties. *New J. Chem.* **2017**, *41*, 4966–4973. [[CrossRef](#)]

11. Li, X.Y.; Chen, L.; Gao, L.; Zhang, Y.; Akogun, S.F.; Dong, W.K. Syntheses, crystal structures and catalytic activities of two solvent-induced homotrinnuclear Co(II) complexes with a naphthalenediol-based bis(Salamo)-type tetraoxime ligand. *RSC Adv.* **2017**, *7*, 35905–35917. [[CrossRef](#)]
12. Song, X.Q.; Wang, L.; Zheng, Q.F.; Liu, W.S. Synthesis, crystal structure and luminescence properties of lanthanide complexes with a new semirigid bridging furfurylsalicylamide ligand. *Inorg. Chim. Acta* **2012**, *391*, 171–178. [[CrossRef](#)]
13. Dong, W.K.; Zhang, J.; Zhang, Y.; Li, N. Novel multinuclear transition metal(II) complexes based on an asymmetric Salamo-type ligand: Syntheses, structure characterizations and fluorescent properties. *Inorg. Chim. Acta* **2016**, *444*, 95–102. [[CrossRef](#)]
14. Gao, L.; Wang, F.; Zhao, Q.; Zhang, Y.; Dong, W.K. Mononuclear Zn(II) and trinuclear Ni(II) complexes derived from a coumarin-containing N<sub>2</sub>O<sub>2</sub> ligand: Syntheses, crystal structures and fluorescence properties. *Polyhedron* **2018**, *139*, 7–16. [[CrossRef](#)]
15. Dong, X.Y.; Kang, Q.P.; Jin, B.X.; Dong, W.K. A dinuclear nickel(II) complex derived from an asymmetric Salamo-type N<sub>2</sub>O<sub>2</sub> chelate ligand: Synthesis, structure and optical properties. *Z. Naturforsch.* **2017**, *72*, 415–420. [[CrossRef](#)]
16. Dong, W.K.; Zhu, L.C.; Ma, J.C.; Sun, Y.X.; Zhang, Y. Two novel mono- and heptanuclear Ni(II) complexes constructed from new unsymmetric and symmetric Salamo-type bisoximes—Synthetic, structural and spectral studies. *Inorg. Chim. Acta* **2016**, *453*, 402–408. [[CrossRef](#)]
17. Liu, P.P.; Wang, C.Y.; Zhang, M.; Song, X.Q. Pentanuclear sandwich-type Zn<sup>II</sup>-Ln<sup>III</sup> clusters based on a new Salen-like salicylamide ligand: Structure, near-infrared emission and magnetic properties. *Polyhedron* **2017**, *129*, 133–140. [[CrossRef](#)]
18. Akine, S.; Taniguchi, T.; Nabeshima, T. Synthesis and Characterization of Novel Ligands 1,2-Bis(salicylideneaminoxy)ethanes. *Chem. Lett.* **2001**, *30*, 682–683. [[CrossRef](#)]
19. Dong, W.K.; Ma, J.C.; Zhu, L.C.; Zhang, Y. Nine self-assembled nickel(II)-lanthanide(III) heterometallic complexes constructed from a Salamo-type bisoxime and bearing N- or O-donor auxiliary ligand: Syntheses, structures and magnetic properties. *New J. Chem.* **2016**, *40*, 6998–7010. [[CrossRef](#)]
20. Dong, W.K.; Li, X.L.; Wang, L.; Zhang, Y.; Ding, Y.J. A new application of Salamo-type bisoximes: As a relay-sensor for Zn<sup>2+</sup>/Cu<sup>2+</sup> and its novel complexes for successive sensing of H<sup>+</sup>/OH<sup>-</sup>. *Sens. Actuators B* **2016**, *229*, 370–378. [[CrossRef](#)]
21. Dong, W.K.; Akogun, S.F.; Zhang, Y.; Sun, Y.X.; Dong, X.Y. A reversible “turn-on” fluorescent sensor for selective detection of Zn<sup>2+</sup>. *Sens. Actuators B* **2017**, *238*, 723–734. [[CrossRef](#)]
22. Wang, B.J.; Dong, W.K.; Zhang, Y.; Akogun, S.F. A novel relay-sensor for highly sensitive and selective detection of Zn<sup>2+</sup>/Pic<sup>-</sup> and fluorescence on/off switch response of H<sup>+</sup>/OH<sup>-</sup>. *Sens. Actuators B* **2017**, *247*, 254–264. [[CrossRef](#)]
23. Wang, F.; Gao, L.; Zhao, Q.; Zhang, Y.; Dong, W.K.; Ding, Y.J. A highly selective fluorescent chemosensor for CN<sup>-</sup> based on a novel bis(salamo)-type tetraoxime ligand. *Spectrochim. Acta A* **2018**, *190*, 111–115. [[CrossRef](#)] [[PubMed](#)]
24. Chen, L.; Dong, W.K.; Zhang, H.; Zhang, Y.; Sun, Y.X. Structural Variation and Luminescence Properties of Tri- and Dinuclear CuII and ZnII Complexes Constructed from a Naphthalenediol-Based Bis(Salamo)-type Ligand. *Cryst. Growth Des.* **2017**, *17*, 3636–3648. [[CrossRef](#)]
25. Li, G.; Hao, J.; Liu, L.Z.; Zhou, W.M.; Dong, W.K. Syntheses, Crystal Structures and Thermal Behaviors of Two Supramolecular Salamo-Type Cobalt(II) and Zinc(II) Complexes. *Crystals* **2017**, *7*, 217.
26. Yang, Y.H.; Hao, J.; Dong, Y.J.; Wang, G.; Dong, W.K. Two Zinc(II) Complexes Constructed from a Bis(salamo)-type Tetraoxime Ligand: Syntheses, Crystal Structures and Luminescence Properties. *Chin. J. Inorg. Chem.* **2017**, *33*, 1280–1292.
27. Chai, L.Q.; Wang, G.; Sun, Y.X.; Dong, W.K.; Zhao, L.; Gao, X.H. Synthesis, crystal structure, and fluorescence of an unexpected dialkoxo-bridged dinuclear copper(II) complex with bis(salen)-type tetraoxime. *J. Coord. Chem.* **2012**, *65*, 1621–1631. [[CrossRef](#)]
28. Zhao, L.; Dang, X.T.; Chen, Q.; Zhao, J.X.; Wang, L. Synthesis, Crystal Structure and Spectral Properties of a 2D Supramolecular Copper(II) Complex With 1-(4-[(E)-3-ethoxyl-2-hydroxybenzylidene]amino)phenyl)ethanone Oxime. *Synth. React. Inorg. Met. Org. Nano Met. Chem.* **2013**, *43*, 1241–1246. [[CrossRef](#)]

29. Zhao, L.; Wang, L.; Sun, Y.X.; Dong, W.K.; Tang, X.L.; Gao, X.H. A supramolecular copper(II) complex bearing salen-type bisoxime ligand: Synthesis, structural characterization, and thermal property. *Synth. React. Inorg. Met. Org. Nano Met. Chem.* **2012**, *42*, 1303–1308. [[CrossRef](#)]
30. Akine, S.; Kagiya, S.; Nabeshima, T. Modulation of Multimetal Complexation Behavior of Tetraoxime Ligand by Covalent Transformation of Olefinic Functionalities. *Inorg. Chem.* **2010**, *49*, 2141–2152. [[CrossRef](#)] [[PubMed](#)]
31. Wang, P.; Zhao, L. An Infinite 2D Supramolecular Cobalt(II) Complex Based on an Asymmetric Salamo-Type Ligand: Synthesis, Crystal Structure, and Spectral Properties. *Synth. React. Inorg. Met. Org. Nano Met. Chem.* **2016**, *46*, 1095–1101. [[CrossRef](#)]
32. Dong, X.Y.; Sun, Y.X.; Wang, L.; Li, L. Synthesis and structure of a penta- and hexa-coordinated tri-nuclear cobalt(II) complex. *J. Chem. Res.* **2012**, *36*, 387–390. [[CrossRef](#)]
33. Wu, H.L.; Pan, G.L.; Bai, Y.C.; Zhang, Y.H.; Wang, H.; Shi, F.R.; Wang, X.L. Study on synthesis, crystal structure, antioxidant and DNA-binding of mono-, di- and poly-nuclear lanthanides complexes with bis(*N*-salicylidene)-3-oxapentane-1,5-diamine. *J. Photochem. Photobiol. B* **2014**, *135*, 33–43. [[CrossRef](#)] [[PubMed](#)]
34. Wu, H.L.; Bai, Y.C.; Zhang, Y.H.; Li, Z.; Wu, M.C.; Chen, C.Y.; Zhang, J.W. Synthesis, crystal structure, antioxidation and DNA-binding properties of a dinuclear copper(II) complex with bis(*N*-salicylidene)-3-oxapentane-1,5-diamine. *J. Coord. Chem.* **2014**, *67*, 3054–3066. [[CrossRef](#)]
35. Chen, C.Y.; Zhang, J.W.; Zhang, Y.H.; Yang, Z.H.; Wu, H.L.; Pan, G.L.; Bai, Y.C. Gadolinium(III) and dysprosium(III) complexes with a Schiff base bis(*N*-salicylidene)-3-oxapentane-1,5-diamine: Synthesis, characterization, antioxidation, and DNA-binding studies. *J. Coord. Chem.* **2015**, *68*, 1054–1071. [[CrossRef](#)]
36. Wu, H.L.; Wang, C.P.; Wang, F.; Peng, H.P.; Zhang, H.; Bai, Y.C. A New Manganese(III) Complex from Bis(5-methylsalicylaldehyde)-3-oxapentane-1,5-diamine: Synthesis, Characterization, Antioxidant Activity and Luminescence. *J. Chin. Chem. Soc.* **2015**, *62*, 1028–1034. [[CrossRef](#)]
37. Wu, H.L.; Bai, Y.C.; Zhang, Y.H.; Pan, G.L.; Kong, J.; Shi, F.R.; Wang, X.L. Two Lanthanide(III) Complexes based on the Schiff Base *N,N'*-Bis(salicylidene)-1,5-diamino-3-oxapentane: Synthesis, Characterization, DNA-binding Properties, and Antioxidation. *Z. Anorg. Allg. Chem.* **2014**, *640*, 2062–2071. [[CrossRef](#)]
38. Dong, W.K.; Ma, J.C.; Dong, Y.J.; Zhu, L.C.; Zhang, Y. Di- and tetranuclear heterometallic 3d–4f cobalt(II)–lanthanide(III) complexes derived from a hexadentate bisoxime: Syntheses, structures and magnetic properties. *Polyhedron* **2016**, *115*, 228–235. [[CrossRef](#)]
39. Song, X.Q.; Liu, P.P.; Xiao, Z.R.; Li, X.; Liu, Y.A. Four polynuclear complexes based on a versatile salicylamide salen-like ligand: Synthesis, structural variations and magnetic properties. *Inorg. Chim. Acta* **2015**, *438*, 232–244. [[CrossRef](#)]
40. Liu, P.P.; Sheng, L.; Song, X.Q.; Xu, W.Y.; Liu, Y.A. Synthesis, structure and magnetic properties of a new one dimensional manganese coordination polymer constructed by a new asymmetrical ligand. *Inorg. Chim. Acta* **2015**, *434*, 252–257. [[CrossRef](#)]
41. Song, X.Q.; Liu, P.P.; Liu, Y.A.; Zhou, J.J.; Wang, X.L. Two dodecanuclear heterometallic [Zn<sub>6</sub>Ln<sub>6</sub>] clusters constructed by a multidentate salicylamide salen-like ligand: Synthesis, structure, luminescence and magnetic properties. *Dalton Trans.* **2016**, *45*, 8154–8163. [[CrossRef](#)] [[PubMed](#)]
42. Song, X.Q.; Zheng, Q.F.; Wang, L.; Liu, W.S. Synthesis and luminescence properties of lanthanide complexes with a new tripodal ligand featuring *N*-thenylsalicylamide arms. *Luminescence* **2012**, *27*, 459–465. [[CrossRef](#)] [[PubMed](#)]
43. Zhang, H.; Dong, W.K.; Zhang, Y.; Akogun, S.F. Naphthalenediol-based bis(Salamo)-type homo- and heterotrimeric cobalt(II) complexes: Syntheses, structures and magnetic properties. *Polyhedron* **2017**, *133*, 279–293. [[CrossRef](#)]
44. Akine, S.; Taniguchi, T.; Dong, W.K.; Masubuchi, S.; Nabeshima, T. Oxime-Based Salen-Type Tetradentate Ligands with High Stability against Imine Metathesis Reaction. *J. Org. Chem.* **2005**, *70*, 1704–1711. [[CrossRef](#)] [[PubMed](#)]
45. Sheldrick, G.M. *SHELXS-97 and SHELXL-97, Fortran Programs for Crystal Structure Solution and Refinement*; University of Gottingen: Gottingen, Germany, 1997.
46. Dong, W.K.; Li, G.; Li, X.; Yang, C.J.; Zhao, M.M.; Dong, X.Y. An Asymmetrical Salamo-type Chelating Ligand with its Cobalt(II) Complex: Syntheses, Characterizations and Crystal Structures. *Chin. J. Inorg. Chem.* **2014**, *30*, 1911–1919.

47. Anthonysamy, A.; Balasubramanian, S. Synthesis, spectral, thermal and electrochemical studies of nickel (II) complexes with N<sub>2</sub>O<sub>2</sub> donor ligands. *Inorg. Chem. Commun.* **2005**, *8*, 908–911. [[CrossRef](#)]
48. Faniran, J.A.; Patel, K.S.; Bailar, J.C. Infrared spectra of N,N'-bis(salicylidene)-1,1-(dimethyl)ethylenediamine and its metal complexes. *J. Inorg. Nucl. Chem.* **1974**, *36*, 1547–1551. [[CrossRef](#)]
49. Wang, L.; Ma, J.C.; Dong, W.K.; Zhu, L.C.; Zhang, Y. A Novel Self-assembled Nickel(II)–Cerium(III) Heterotetranuclear Dimer Constructed from N<sub>2</sub>O<sub>2</sub>-type Bisoxime and Terephthalic Acid: Synthesis, Structure and Photophysical Properties. *Z. Anorg. Allg. Chem.* **2016**, *642*, 834–839. [[CrossRef](#)]
50. Wang, L.; Li, X.Y.; Zhao, Q.; Li, L.H.; Dong, W.K. Fluorescence properties of heterotrinnuclear Zn(II)–M(II) (M = Ca, Sr and Ba) bis(salamo)-type complexes. *RSC Adv.* **2017**, *7*, 48730–48737. [[CrossRef](#)]
51. Xu, L.; Zhu, L.C.; Ma, J.C.; Zhang, Y.; Zhang, J.; Dong, W.K. Syntheses, structures and spectral properties of mononuclear Cu<sup>II</sup> and dimeric Zn<sup>II</sup> complexes based on an asymmetric Salamo-type N<sub>2</sub>O<sub>2</sub> ligand. *Z. Anorg. Allg. Chem.* **2015**, *641*, 2520–2524. [[CrossRef](#)]
52. Dong, X.Y.; Li, X.Y.; Liu, L.Z.; Zhang, H.; Ding, Y.J.; Dong, W.K. Tri- and hexanuclear heterometallic Ni(II)–M(II) (M = Ca, Sr and Ba) bis(salamo)-type complexes: Synthesis, structure and fluorescence properties. *RSC Adv.* **2017**, *7*, 48394–48403. [[CrossRef](#)]
53. Chai, L.Q.; Tang, L.J.; Chen, L.C.; Huang, J.J. Structural, spectral, electrochemical and DFT studies of two mononuclear manganese(II) and zinc(II) complexes. *Polyhedron* **2017**, *122*, 228–240. [[CrossRef](#)]
54. Sun, Y.X.; Gao, X.H. Synthesis, characterization, and crystal structure of a new CuII complex with salen-type ligand. *Synth. React. Inorg. Met. Org. Nano Met. Chem.* **2011**, *41*, 973–978. [[CrossRef](#)]
55. Dong, W.K.; Zhang, J.T.; Dong, Y.J.; Zhang, Y.; Wang, Z.K. Construction of Mononuclear Copper(II) and Trinuclear Cobalt(II) Complexes Based on Asymmetric Salamo-Type Ligands. *Z. Anorg. Allg. Chem.* **2016**, *642*, 189–196. [[CrossRef](#)]
56. Li, X.Y.; Kang, Q.P.; Liu, L.Z.; Ma, J.C.; Dong, W.K. Trinuclear Co(II) and Mononuclear Ni(II) Salamo-Type Bisoxime Coordination Compounds. *Crystals* **2018**, *8*, 43. [[CrossRef](#)]
57. Hao, J.; Liu, L.Z.; Dong, W.K.; Zhang, J.; Zhang, Y. Three multinuclear Co(II), Zn(II) and Cd(II) complexes based on a single-armed salamo-type bisoxime: Syntheses, structural characterizations and fluorescent properties. *J. Coord. Chem.* **2017**, *70*, 1936–1952. [[CrossRef](#)]
58. Gao, L.; Liu, C.; Wang, F.; Dong, W.K. Tetra-, Penta- and Hexa-Coordinated Transition Metal Complexes Constructed from Coumarin-Containing N<sub>2</sub>O<sub>2</sub> Ligand. *Crystals* **2018**, *8*, 77. [[CrossRef](#)]
59. Dong, W.K.; Zheng, S.S.; Zhang, J.T.; Zhang, Y.; Sun, Y.X. Luminescent properties of heterotrinnuclear 3d–4f complexes constructed from a naphthalenediol-based acyclic bis(salamo)-type ligand. *Spectrochim. Acta A* **2017**, *184*, 141–150. [[CrossRef](#)] [[PubMed](#)]
60. Chai, L.Q.; Huang, J.J.; Zhang, H.S.; Zhang, Y.L.; Zhang, J.Y.; Li, Y.X. An unexpected cobalt(III) complex containing a Schiff base ligand: Synthesis, crystal structure, spectroscopic behavior, electrochemical property and SOD-like activity. *Spectrochim. Acta A* **2014**, *131*, 526–533. [[CrossRef](#)] [[PubMed](#)]
61. Wang, L.; Hao, J.; Zhai, L.X.; Zhang, Y.; Dong, W.K. Synthesis, Crystal Structure, Luminescence, Electrochemical and Antimicrobial Properties of Bis(salamo)-Based Co(II) Complex. *Crystals* **2017**, *7*, 277. [[CrossRef](#)]
62. Dong, X.Y.; Gao, L.; Wang, F.; Zhang, Y.; Dong, W.K. Tri- and Mono-Nuclear Zinc(II) Complexes Based on Half- and Mono-Salamo Chelating Ligands. *Crystals* **2017**, *7*, 267. [[CrossRef](#)]
63. Chai, L.Q.; Zhang, K.Y.; Tang, L.J.; Zhang, J.Y.; Zhang, H.S. Two mono- and dinuclear Ni(II) complexes constructed from quinazoline-type ligands: Synthesis, X-ray structures, spectroscopic, electrochemical, thermal, and antimicrobial studies. *Polyhedron* **2017**, *130*, 100–107. [[CrossRef](#)]
64. Hao, J.; Li, L.L.; Zhang, J.T.; Akogun, S.F.; Wang, L.; Dong, W.K. Four homo- and hetero-bimetallic 3d/3d-2s complexes constructed from a naphthalenediol-based acyclic bis(salamo)-type tetraoxime ligand. *Polyhedron* **2017**, *134*, 1–10. [[CrossRef](#)]
65. Tao, C.H.; Ma, J.C.; Zhu, L.C.; Zhang, Y.; Dong, W.K. Heterobimetallic 3d–4f Zn(II)–Ln(III) (Ln = Sm, Eu, Tb and Dy) complexes with a N<sub>2</sub>O<sub>4</sub> bisoxime chelate ligand and a simple auxiliary ligand Py: Syntheses, structures and luminescence properties. *Polyhedron* **2017**, *128*, 38–45. [[CrossRef](#)]
66. Dong, W.K.; Zhu, L.C.; Dong, Y.J.; Ma, J.C.; Zhang, Y. Mono, di and heptanuclear metal(II) complexes based on symmetric and asymmetric tetradentate Salamo-type ligands: Syntheses, structures and spectroscopic properties. *Polyhedron* **2016**, *117*, 148–154. [[CrossRef](#)]

67. Wang, P.; Zhao, L. Synthesis, structure and spectroscopic properties of the trinuclear cobalt(II) and nickel(II) complexes based on 2-hydroxynaphthaldehyde and bis(aminooxy)alkane. *Spectrochim. Acta A* **2015**, *135*, 342–350. [[CrossRef](#)] [[PubMed](#)]
68. Sun, Y.X.; Wang, L.; Dong, X.Y.; Ren, Z.L.; Meng, W.S. Synthesis, Characterization, and Crystal Structure of a Supramolecular Co<sup>II</sup> Complex Containing Salen-Type Bisoxime. *Synth. React. Inorg. Met. Org. Nano Met. Chem.* **2013**, *43*, 599–603. [[CrossRef](#)]
69. Song, X.Q.; Cheng, G.Q.; Wang, X.R.; Xu, W.Y.; Liu, P.P. Structure-based description of a step-by-step synthesis of heterodinuclear Zn<sup>II</sup>Ln<sup>III</sup> complexes and their luminescence properties. *Inorg. Chim. Acta* **2015**, *425*, 145–153. [[CrossRef](#)]
70. Dong, Y.J.; Ma, J.C.; Zhu, L.C.; Dong, W.K.; Zhang, Y. Four 3d–4f heteromultinuclear zinc(II)–lanthanide(III) complexes constructed from a distinct hexadentate N<sub>2</sub>O<sub>2</sub>-type ligand: Syntheses, structures and photophysical properties. *J. Coord. Chem.* **2017**, *70*, 103–115. [[CrossRef](#)]
71. Dong, W.K.; Lan, P.F.; Zhou, W.M.; Zhang, Y. Salamo-type trinuclear and tetranuclear cobalt(II) complexes based on a new asymmetry Salamotype ligand: Syntheses, crystal structures, and fluorescence properties. *J. Coord. Chem.* **2016**, *69*, 1272–1283. [[CrossRef](#)]
72. Costes, J.P.; Maurice, R.; Vendier, L. Pentacoordinate Ni<sup>II</sup> Complexes: Preparation, Magnetic Measurements, and Ab Initio Calculations of the Magnetic Anisotropy Terms. *Chem. Eur. J.* **2012**, *18*, 4031–4040. [[CrossRef](#)] [[PubMed](#)]
73. Mandal, D.; Chatterjee, P.B.; Ganguly, R.; Tiekink, E.R.T.; Clérac, R.; Chaudhury, M. Tetra- and Dinuclear Nickel(II)–Vanadium(IV/V) Heterometal Complexes of a Phenol-Based N<sub>2</sub>O<sub>2</sub> Ligand: Synthesis, Structures, and Magnetic and Redox Properties. *Inorg. Chem.* **2008**, *47*, 584–591. [[CrossRef](#)] [[PubMed](#)]
74. Mandal, D.; Chatterjee, P.B.; Bhattacharya, S.; Choi, K.-Y.; Clérac, R.; Chaudhury, M. Tetra-, Tri-, and Mononuclear Manganese(II/III) Complexes of a Phenol-Based N<sub>2</sub>O<sub>2</sub> Capping Ligand: Use of Carboxylates as Ancillary Ligands in Tuning the Nuclearity of the Complexes. *Inorg. Chem.* **2009**, *48*, 1826–1835. [[CrossRef](#)] [[PubMed](#)]



© 2018 by the authors. Licensee MDPI, Basel, Switzerland. This article is an open access article distributed under the terms and conditions of the Creative Commons Attribution (CC BY) license (<http://creativecommons.org/licenses/by/4.0/>).